



Effects of organic solvents and different aqueous-phase additives on the polyamide (PA) thin-film composite (TFC) membranes for forward osmosis

Zhixia Liang^a, Yanbin Yun^{a,*}, Quanju Ji^a, Qiang Xia^a, Chunli Li^b

^aSchool of Environmental Science and Engineering, Beijing Forestry University, Beijing, 100083, China,

emails: yunyanbin@bjfu.edu.cn (Y. Yun), liangzhixia6@126.com (Z. Liang), quanju_ji@126.com (Q. Ji), xq7717@126.com (Q. Xia)

^bNew Technique Centre, Institute of Microbiology, Chinese Academy of Sciences, Beijing, 100101, China, email: licl@im.ac.cn

Received 26 July 2017; Accepted 19 February 2018

ABSTRACT

Forward osmosis (FO) membranes have gained increasing attention due to their potential advantages such as low fouling propensity, low energy consumption and high recovery. In this study, an investigation about the effect of polyamide (PA) structure on performance of the thin-film composite (TFC) FO membranes in the interfacial polymerization has been carried out systematically. Four organic solvents and aqueous-phase additives are selected to produce the thin-film membranes, the properties of which such as morphology, hydrophilicity, crosslinking degree and FO performance were evaluated. Among the four types of organic solvents, the hexane-based PA TFC membrane shows the highest water permeability, hydrophilicity and the lowest crosslinking degree. Meanwhile, the TFC membranes with high boiling point solvents (heptane and isopar) exhibit high water flux at high curing temperature, which is different from the low boiling point solvents (hexane and cyclohexane). Furthermore, four kinds of additives in aqueous phase were introduced to form desired PA layers. FO performance of PA TFC membranes was improved with the addition of dimethyl sulfoxide (DMSO) and N,N-dimethylformamide (DMF) by reducing the solubility difference of the two immiscible phase and facilitating the diffusion of 1,3-phenylenediamine into the organic 1,3,5-benzenetricarbonyl trichloride phase. In general, the hexane-based PA TFC membrane with the 3 wt% DMSO as an additive shows a much better FO performance.

Keywords: Thin-film composite membrane; Polyamide; Interfacial polymerization; Forward osmosis

1. Introduction

Membrane separation processes are now the primary technology used in wastewater reclamation and desalination [1]. Over the past decade, forward osmosis (FO) process has attracted worldwide interest in the field of desalination and wastewater treatment to meet the growing demand of fresh water. This is mainly ascribed to its low fouling propensity, low energy consumption and high recovery [2]. In general, FO thin-film composite (TFC) membrane consists of an ultra-thin polyamide (PA) active layer and a porous substrate. The substrate provides strength to the PA layer and maintains

membrane's integrity in FO processes [3]. Though both the layers (substrate and PA layer) can be independently optimized with respect to strength, stability and performance, the properties of the PA layer are important factors for the membrane separation efficiencies [4].

Interfacial polymerization (IP) is the most commonly used technique for preparing PA TFC membrane, which was introduced by Sasaki et al. [5]. In this technique, the PA layer is produced on the porous substrate by reacting with two monomers, 1,3-phenylenediamine monomer taken in water and 1,3,5-benzenetricarbonyl trichloride taken in hexane solvent, and the polymerization reaction takes place at the interface [6,7]. In recent literatures, many researches have been focused on fabrication of high-performance TFC

* Corresponding author.

membranes by optimizing structure of the PA active layer via the IP reaction [8–11]. In general, the IP reaction includes some key parameters, for example, the types of monomers and organic solvents, aqueous-phase additives and heat-treating process [12–18]. The TFC RO membrane with heptane as the organic solvent heat-treated at 75°C has higher water permeability, lower roughness and excellent salt rejection compared with other organic solvents [19]. There have been reports on utilization of a co-solvent such as isopropanol (IPA) and N,N-dimethylformamide (DMF) into the organic phase to enhance the miscibility at the interface and showed significantly lower rejection and higher flux than that of membranes with no additives [20]. The effect of organic solutions on the performance of PA TFC nanofiltration membranes was investigated and demonstrated that isopar was suitable for increasing the rejection rate compared with hexane [21]. It is critical to select organic solvents with high surface tension but low viscosity, since which governs the amine monomer prolongation and aromatic acyl chloride hydrolysis during IP reaction [19]. Cyclohexane, heptane, isopar and hexane as the most commonly used organic solvents in interfacial polymerization were studied in this paper [16–21].

In addition, during the IP reaction, the pH of the solution decreases first due to the consumption of amines and second due to the formation of hydrochloric acid as a result of reaction between diamines and acid chloride [4]. Hence, some acid acceptor (e.g., triethylamine, sodium hydroxide, sodium tertiary phosphate, dimethyl piperazine and camphor sulfonic acid) was added in the aqueous phase to accelerate the IP reaction [22–27]. Adding hydrophilic water-soluble polymers such as N,N-dimethylformamide, dimethyl sulfoxide to the amine solution can produce high-flux reverse osmosis membranes with good rejection [28–30]. The addition of lithium bromide (LiBr) and sodium dodecyl sulfate (SDS) in 1,3-phenylenediamine (MPD) solution was found to facilitate the reaction between the two phases and resulted in a significant improvement in water permeability [31]. However, these studies mainly focused on the influence of one or two additives on PA TFC membranes, lacking of systematic research for the effect of typical additives on the performance of the PA TFC membranes.

In this work, fabrication of PA TFC membranes for FO process was conducted through controlling the preparation parameters of the PA layer with four different organic solvents and four aqueous-phase additives. The PA layer properties in terms of water and salt permeability, contact angle, functional group, surface energy and surface morphology were systematically investigated. To the best of our knowledge, this is the first report on the systematical study of the effect of organic solvents and additives on PA layer properties for TFC FO membranes.

2. Materials and methods

2.1. Materials

Polysulfone (PSf, Mn: 26,000 Da), N-methyl pyrrolidone (NMP, anhydrous, 99.5%), PEG 400 (powder, 99%) and LiCl (powder, 99%) were used for PSf porous substrates. Chemicals used in PA active layer formation included MPD (99%), 1,3,5-benzenetricarbonyl trichloride

(TMC, 98%), and aqueous solution additives (e.g., triethylamine [TEA; liquid, 99.5%], dimethyl sulfoxide [DMSO; liquid, 99%], N,N-dimethylformamide [DMF; liquid, 99%], piperazine hexahydrate [PIP; powder, 99%] and isopropanol [IPA; liquid, 99%]). There are four organic solvents used to prepare the TMC solution, included hexane (Beijing Chemical Works [Beijing, China], 95%), heptane (Beijing Chemical Works [Beijing, China], 95%), cyclohexane (Beijing Chemical works [Beijing, China], 95%) and isopar-G (isopar, a proprietary nonpolar organic solvent, Univar, Redmond, WA, 99%). Sodium chloride (NaCl, crystals, ACS reagent, Sinopharm Chemical Reagent Co., Ltd. [Beijing, China]) was dissolved in deionized (DI) water obtained from a Milli-Q ultra-pure water purification system (Millipore, Billerica, MA).

2.2. Membrane preparation

2.2.1. Preparation of PSf substrates

PSf substrate was prepared according to the usual phase inversion method by dissolving 12 g PSf beads, 4 g PEG 400 and 2 g LiCl in 82 g of NMP solvent. Prior to membrane casting, the solution was stirred at room temperature for 8 h and then stored in a desiccator for at least 15 h. A 100 μm casting knife was used to spread the PSf solution onto a glass plate. Then the substrate was immediately immersed in DI water at room temperature to initiate the phase inversion. The obtained PSf substrate was then stored in a DI water bath for the following IP reaction.

2.2.2. Preparation of PA rejection layer

The PA rejection layer was prepared via IP process on the surface of the PSf substrate. First, the PSf substrate was immersed in a 3.4 wt% MPD aqueous solution with different additives (e.g., triethylamine [TEA], dimethyl sulfoxide [DMSO], dimethylformamide [DMF] and piperazine [PIP]) for 120 s. An air knife was then used to remove excess MPD solution off the membrane surface. Then, the MPD-saturated substrate was immersed into the different organic phase 0.15 wt% TMC solution (i.e., hexane, heptane, cyclohexane and isopar) for 60 s, resulting in the formation of an ultra-thin PA layer. The composite membranes were cured in DI water at 65°C for 120 s (unless otherwise specified), then rinsed with a 200 ppm NaClO (available chlorine 8%–12%) aqueous solution for 120 s, followed by rinsing for 30 s with 1,000 ppm NaHSO₃ aqueous solution, before final heat-curing step at 65°C for 120 s. The fabricated TFC membranes were rinsed thoroughly and stored in DI water at 4°C.

2.3. Evaluation of FO performance

FO experiments were conducted with a lab-scale cross-flow filtration unit, as illustrated in Fig. 1. The cross-flow filtration unit included a cell with 40 cm² effective membrane (length 10 cm, width 4 cm). 1 M NaCl solution was used as draw solution (DS) and DI water as feed. Temperatures of the feed and DSs were maintained at 25°C \pm 0.5°C. The feed solution (FS) and DS were circulated on each side of the membrane at a cross-flow rate of

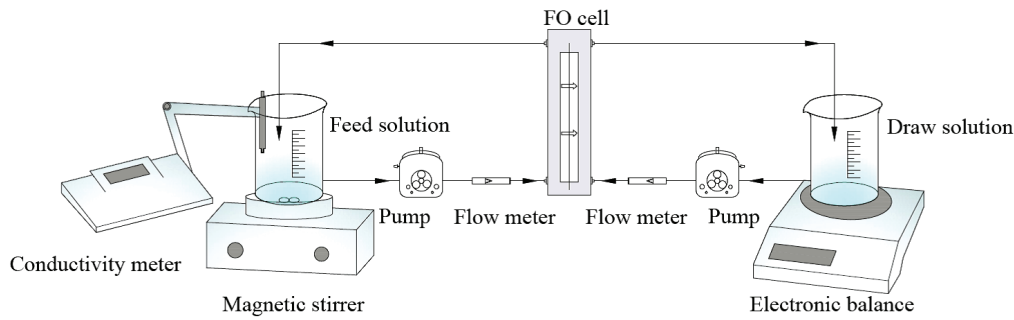


Fig. 1. Lab-scale forward osmosis testing system.

0.013 m s^{-1} , which was controlled by flow meter and magnetic pumps (MP-20RM, Shanghai Xinxishan Industrial Co., Ltd. [Shanghai, China]). Membranes were tested under FO mode where FS faces the PA layer. The test was conducted for 1 h in triplicate. The reverse salt flux could be calculated with measured conductivity (DDSJ-308F, INESA Scientific Instrument Co., Ltd. [Shanghai, China]) of the FS at the end of the experiment. Mass change of permeated water over time was recorded by a balance (HZT-A2000, Huazhi Scientific Instrument Co., Ltd. [Fujian, China]). The water flux (J_w , $\text{L m}^{-2} \text{ h}^{-1}$) refers to the volume of pure water transferred from FS to DS per unit area and per unit time, which was calculated as follows:

$$J_w = \frac{\Delta V}{A \Delta t} \quad (1)$$

where ΔV (L) is the volume change of the DS over a predetermined time Δt (h) and A is the effective membrane surface area (m^2).

The salt reverse flux (J_s , $\text{g m}^{-2} \text{ h}^{-1}$) was defined as the quality of NaCl diffusing from the DS to the FS per unit membrane area per unit time and determined by the conversion of its electrical conductivity measured by a conductivity meter. It was calculated as follows:

$$J_s = \frac{V_t C_t - V_0 C_0}{A \Delta t} \quad (2)$$

where C_t and V_t are the concentration and volume of the FS measured over a predetermined time Δt (h), and C_0 and V_0 are the initial concentration and initial volume of the FS, respectively. A (m^2) is the available membrane area, Δt (h) is the effective testing time. The salt quality was calculated by using the standard curve established before experiments.

2.4. Characterization of the membranes

The surface was observed using scanning electron microscopy (SEM, FEI, Quanta 200, Holland). Before the observation, membranes were fractured in liquid nitrogen, and coated with gold using a sputtering coater (MC1000 Ion Sputter). Attenuated total reflectance-Fourier transform infrared spectroscopy (ATR-FTIR, Vertex 70, Bruker [Ettlingen, Germany]) was used to identify the functional groups of

the PA active layer and analyze the chemical changes of the PA layer. Surface hydrophilicity of the TFC membrane was determined by contact angle instrument (JY-PHa, Chengde Jinhe Instrument Manufacturing Co., Ltd. [Hebei, China]) using sessile drop method. For each membrane type, three different samples were tested in 12 random locations. A $2 \mu\text{L}$ droplet was placed on a freeze-dried membrane surface, and contact angles were measured. The interfacial tension between a condensed-phase material and water is one of the most important terms occurring (directly or indirectly) in the major surface thermodynamic combining rules, the equations for the free energies of interaction between apolar or polar entities, immersed in water was evaluated by Young–Dupré equation, which forms the link between contact angles (θ) of a drop of liquid (L) deposited on a flat solid surface (S), with the surface tension of the liquid (γ_L) and the solid (γ_S); γ^{LW} was designated as the apolar part of the surface tension; the parameter γ_S^+ and γ_L^+ represented its electron-acceptivity as well as γ_S^- and γ_L^- represented its electron-donicity [28]. In conjunction with the surface tension values of water, γ^{LW} , γ_S^+ , γ_S^- of the membrane can be calculated from the solution of Eqs. (3) and (4):

$$(1 + \cos\theta)\gamma_L = -\Delta G_{\text{SL}} \quad (3)$$

$$-\Delta G_{\text{SL}} = 2\left(\sqrt{\gamma_S^{\text{LW}}\gamma_L^{\text{LW}}} + \sqrt{\gamma_S^+\gamma_L^-} + \sqrt{\gamma_S^-\gamma_L^+}\right) \quad (4)$$

The Lewis acid–base system describes the electron-acceptivity (Lewis acid) and electron-donicity (Lewis base) of polar materials and the Lifshitz–van der Waals property designated as the apolar part of the surface tension, in terms of γ^{LW} , one can describe the entire polar part of the surface tension of that material as γ^{AB} (acid–base), which is equally true for γ_L [32,33].

$$\gamma_S = \gamma_S^{\text{LW}} + \gamma_S^{\text{AB}} \quad (5)$$

$$\gamma_S^{\text{AB}} = 2\sqrt{\gamma_S^+\gamma_S^-} \quad (6)$$

where the subscripts S and L refer to the membrane and liquid, respectively. The interfacial free energy and surface energy of the membranes were analyzed by the contact

angle method with two polar liquids, water and glycerol, and an apolar liquid, diiodomethane, the surface tension of which was assumed as 72.8, 64.0 and 50.8 mJ m⁻² at room temperature, respectively [34,35]. Using the surface tension components of membrane and water, the interfacial free energy of cohesion of membrane interfaces immersed in water was also calculated [36–38].

2.5. Determination of transport and structural parameters

The water and solute permeability coefficients (A and B , respectively) and structural parameters (S) are three intrinsic parameters that fully describe membrane system and can be used with the respective governing equations to accurately predict the water and salt flux performance of a membrane sample in any laboratory-scale FO system. The three parameters were characterized by adopting the Excel-based algorithm developed by Tiraferri et al. [39]. The simultaneous determination of A , B and S parameters of FO membranes was obtained through Eqs. (7) and (8), where a single FO experiment including four stages was conducted, each stage of that used different concentration of DS (500; 1,000; 1,500; 2,000 mM) with a DI water FS.

$$J_w = A \left\{ \frac{\pi_D \exp\left(-\frac{J_w S}{D}\right) - \pi_F}{1 + \frac{B}{J_w} \left[1 - \exp\left(-\frac{J_w S}{D}\right) \right]} \right\} \quad (7)$$

$$J_s = B \left\{ \frac{C_D \exp\left(-\frac{J_w S}{D}\right) - C_F}{1 + \frac{B}{J_w} \left[1 - \exp\left(-\frac{J_w S}{D}\right) \right]} \right\} \quad (8)$$

where D is the bulk diffusion coefficient of the draw salt, π_D and π_F are the osmotic pressures for the draw and FSs, and C_D and C_F are the concentrations of the draw solutions and FSs, respectively. In this method, the water and salt flux sets with a low coefficient of variation for the J_w/J_s ratio (10%) and a high coefficient of determination (>0.95) for the water flux (R^2_w) and salt flux (R^2_s) to obtain results close to their true values. A/B was termed as the reverse flux selectivity, and regarded as a quality control parameter [40].

3. Results and discussion

3.1. Morphology and properties of PA TFC membranes with different organic solvents

Fig. 2 shows the surface morphology of the PA TFC membranes with four different solvents. This observation is consistent with the typical characteristic of an interracially polymerized PA membrane prepared by MPD and TMC, which consists of “ridge-and-valley” morphology [41,42]. The cyclohexane membrane (Fig. 3(a)) shows dispersed piece structure consisted of the crooked, worm-like strands connected with each other. Fig. 3(b) shows the surface of the

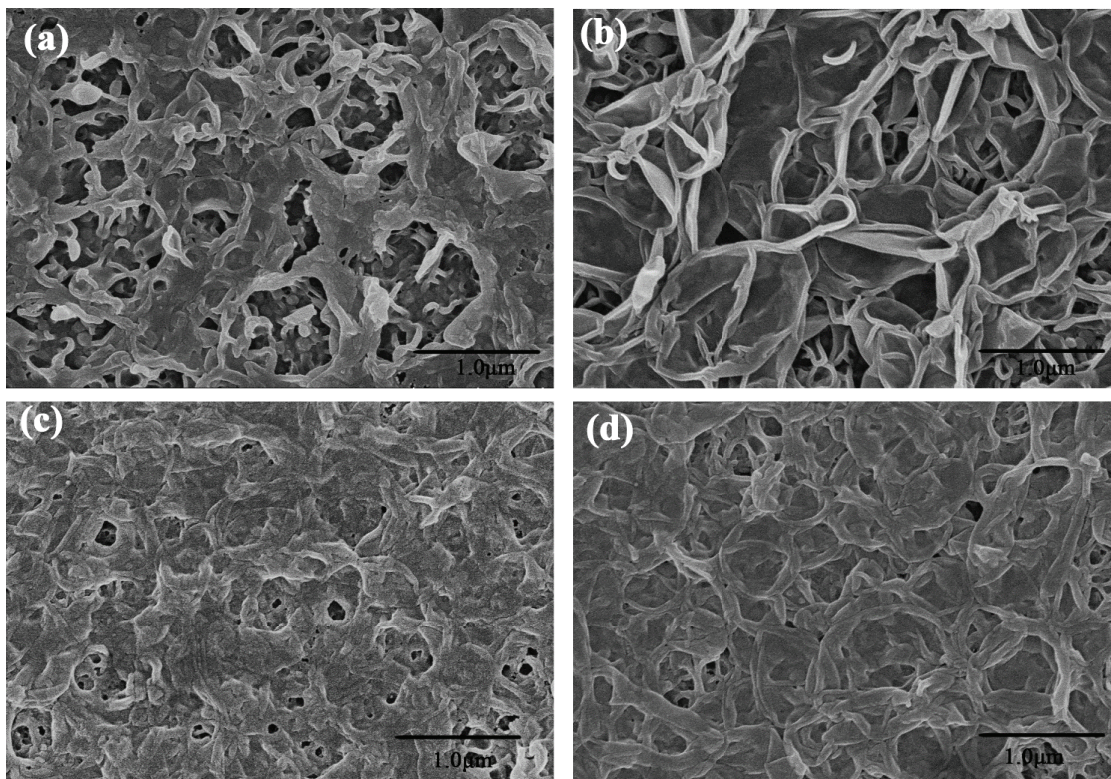


Fig. 2. SEM images of the top surface of PA TFC membrane with four different solvents (a) cyclohexane, (b) heptane, (c) isopar and (d) hexane.

PA TFC membrane with heptane; three-dimensional network structure is visible and obtains higher surface energy compared with other membranes, which indicates that the surface roughness also affect the membrane hydrophilicity [43]. The surface tension of organic solvents controls the MPD solubility and the miscibility of the two liquid phases, hexane shows higher MPD diffusivity and lower MPD solubility among those organic solvents [19]. The films formed by enhancing MPD diffusivity and reducing MPD solubility

tends to increase crosslinking. Based on the obtained data, it is reasonable to conclude that the organic solvents affect the degree of polymerization, the surface morphology and hydrophilicity [44,45].

Table 1 shows the water and salt permeability, structural parameter, hydrophilicity and surface energy of the TFC membranes with four different solvents (heat-treated at 65°C). The hexane films obtained relatively higher water and salt permeability as well as structural parameter, while the membranes with isopar showed lower water permeability and parameters, indicating the type of solvents significantly influenced the performance of TFC membrane. Membranes with hydrophilic surfaces are well known for their high bio-fouling resistance characteristics [19]. Contact angle analysis using the sessile drop method was used to compare the surface hydrophilicity of TFC membranes with four different solvents. As shown in Table 1, the hexane-based PA layer showed better hydrophilicity ($\theta = 79.55^\circ \pm 0.85^\circ$) and higher surface energy ($-\Delta G_{SL} = 41.41 \text{ mJ m}^{-2}$) compared with others. Moreover, the lowest surface energy (19.32 mN m^{-1}) was obtained for cyclohexane-based PA layer.

The changes in surface functional groups of the TFC membranes were investigated by ATR-FTIR as shown in Fig. 3. The TFC membrane spectra disclosed the characteristic peaks of the PA layer formed by the interfacial polymerization of MPD and TMC monomers at $1,661 \text{ cm}^{-1}$ (C=O of amide), $1,610 \text{ cm}^{-1}$ (aromatic ring breathing), and $1,544 \text{ cm}^{-1}$ (C–N stretch of amide II), indicating the successful formation of the PA layer on the top of PSf substrate [39,46]. The weak peak at $1,724 \text{ cm}^{-1}$ corresponds to the C=O stretching of carboxylic acid arising from the hydrolysis of the unreacted acyl chloride [47]. The degree of crosslinking can be roughly estimated from the ratio of the peak intensity at $1,724$ and $1,661 \text{ cm}^{-1}$ ($I_{(-\text{COOH})}/I_{(-\text{CONH})}$) [24]. The variation of the $I_{(-\text{COOH})}/I_{(-\text{CONH})}$ ratio indicated the IP reaction was strongly influenced by the four different solvents as shown in Fig. 3(b). The hexane-based PA layer obtained the lowest $I_{(-\text{COOH})}/I_{(-\text{CONH})}$ ratio. This observation can be explained as the relatively higher solubility and diffusivity of MPD in the hexane, which might alter hydrolysis and the degree of crosslinking [28]. While the isopar-based PA layer had the highest $I_{(-\text{COOH})}/I_{(-\text{CONH})}$ ratio. The faster solution and diffusion of MPD to TMC solvents produced thinner and more crosslinked PA layer, and monomers can more easily form multiple amide linkages [17].

Fig. 4 compares the FO performance of the TFC membranes with different types of organic solvents at different heat-treating temperatures. The organic solvents and heat-treating temperature affect the performance of the TFC membranes. As shown in Fig. 4(a), the water flux of hexane and cyclohexane membranes decreased with the increase of

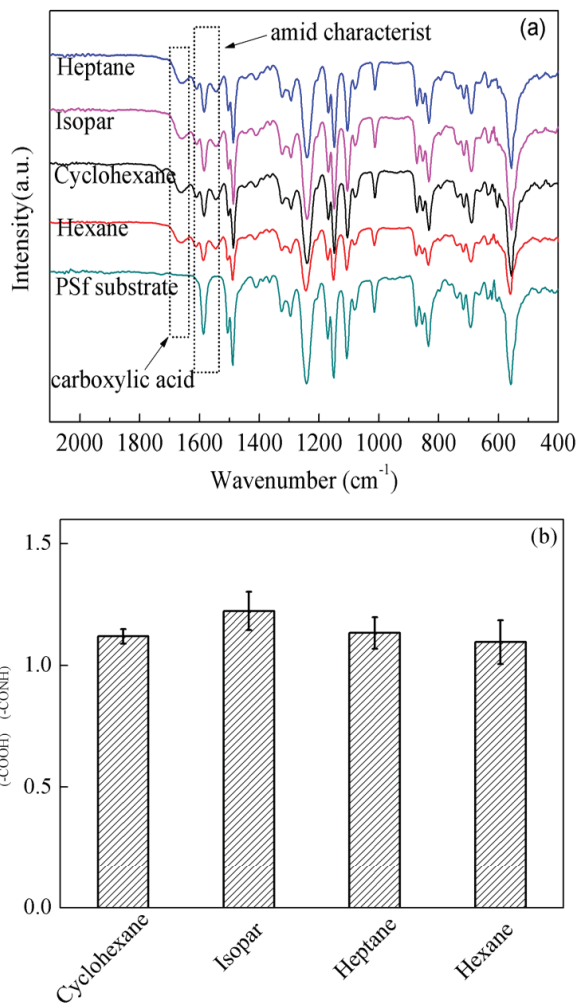


Fig. 3. (a) ATR-FTIR spectra and (b) the estimated ratio of $(-\text{COOH})/(-\text{CONH})$ groups of the PA TFC membranes with four different solvents (heat-treating at 65°C).

Table 1

Analysis of the water permeability (A), salt permeability (B), structural parameter (S), hydrophilicity and surface energy of the TFC membranes with four different solvents

Solvent type	A ($\text{L m}^{-2} \text{h}^{-1} \text{bar}^{-1}$)	B ($\text{L m}^{-2} \text{h}^{-1}$)	S (μm)	Contact angle (deg)	$-\Delta G_{SL}$ (mJ m^{-2})	γ_s^{LW} (mN m^{-1})
Hexane	0.638	0.161	363	79.55 ± 0.85	41.41	24.84
Heptane	0.488	0.148	319	82.79 ± 0.91	36.89	20.99
Cyclohexane	0.587	0.142	276	83.12 ± 1.12	34.63	19.32
Isopar	0.292	0.173	212	83.90 ± 1.24	33.69	24.41

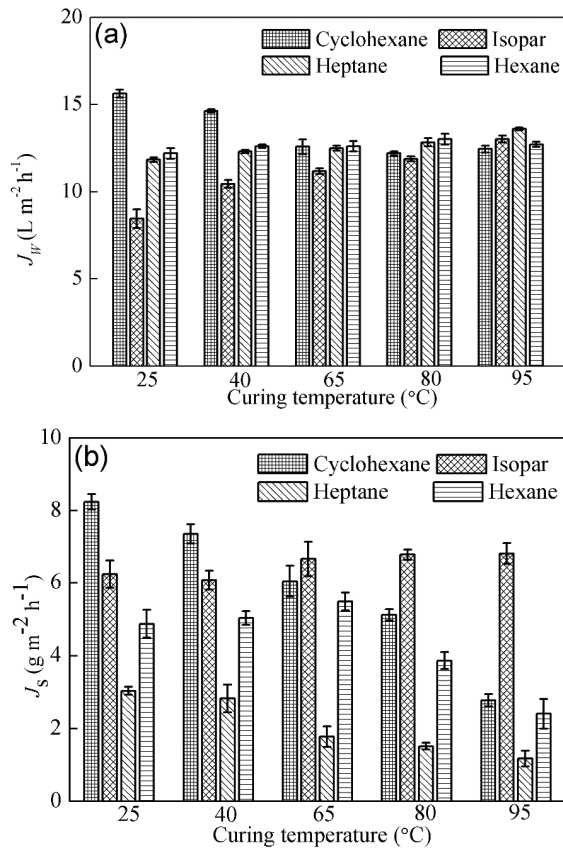


Fig. 4. Performance of TFC membranes with different types of solvent at five heat-treating temperatures. (a) Water flux, (b) reverse salt flux.

heat treatment temperature. This phenomenon is due to that hexane and cyclohexane as low boiling point solvents had been fully removed above 65°C. Once evaporation of organic solvents from the membrane surface is complete, evaporation of bound water inside the membrane occurs, excessive heat may affect the pore size of the PSf substrates, thus resulting in a decrease of the desired flux rate of the membrane [48,49]. This contrasts with the high boiling solvents (heptane and isopar), which exhibit increasing water flux through 90°C. In addition, it was worth to note that the reverse salt flux (Fig. 4(b)) of the PA membranes decreased above 65°C except the isopar-based TFC membrane. It seems a curing temperature above 65°C will provide the desired and stable membranes with low boiling solvents, unlike isopar-based TFC membranes, which can stand high curing temperature [50].

3.2. Morphology and properties of PA TFC membranes with different additives in MPD solution

The additives in MPD solution were used to influence monomer solubility, diffusivity and scavenge inhibitory reaction byproducts. Adding small amounts of hydrophilic water-soluble polymers such as DMSO and DMF to the aqueous amine solution can increase the miscibility of water and hexane and probably also enhance MPD diffusivity, thus, producing high-flux thinner PA film with good rejection [28,51]. The surface morphology of TFC membranes with different additives in MPD solution is displayed in Fig. 5. Compared with the surface of the membranes with DMF and DMSO (Figs. 5(b) and (c)), the TEA-based membranes exhibit smoother structures with worm-like and crooked strands. The addition of PIP to the PA TFC membranes leads to different surface morphology, the surface of the membrane looks open with a larger patch-like structure (Fig. 5(d)). When the

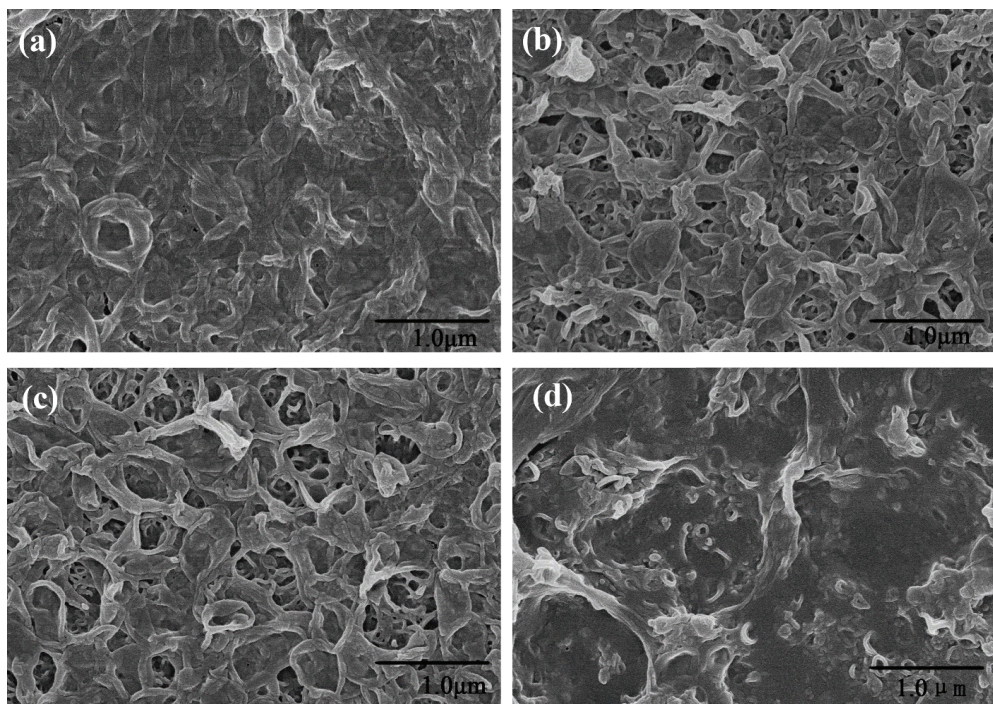


Fig. 5. SEM images of the top surface of PA TFC membrane with 1 wt% additives. (a) TEA, (b) DMF, (c) DMSO and (d) PIP.

reactant amine is a mixture of MPD and PIP, the local amine-TMC reaction rate varies due to the different reactivity and mobility of the amine sites in small molecules of PIP and macromolecules of MPD, resulting in rough surfaces with obvious ridge-valley [51,52].

Table 2 analyzed the membrane characteristics, contact angle, interfacial free energy and surface energy of the TFC membranes with different additives in MPD solution. In general, the introduction of additives except PIP can improve the water permeability in different degrees. The TFC membranes with additives have more satisfactory performance in decreasing solute reverse diffusion and structural parameter (S). Since the effect of ICP can be minimized by reducing S value, it is found that improving the TFC membrane characteristics through incorporation of additives is a reliable strategy to improve the membrane efficiency in FO applications. Generally, the contact angle of the TFC membranes decreases compared with the membranes without additives, and the contact angle of the membrane formed with TEA decreased from 79.55° to 64.07° and the interfacial free energy increased from 41.41 to 59.36 mJ m^{-2} , which was due to that the addition of TEA solvent accelerated the IP reaction by controlling the reaction pH and removing hydrogen halides formation [53]. These results demonstrate that the hydrophilicity of the TFC membranes with additives is significantly improved.

Fig. 6 shows the performance of the TFC membranes with varying amounts of additives. The DMSO and DMF membranes exhibited higher water flux compared with others, which have a Hildebrand solubility parameters (24.8 and $26.6 \text{ MPa}^{1/2}$) between those of water and hexane, thereby reducing the solubility difference of the two immiscible phase and facilitating the diffusion of MPD into the organic TMC phase [54]. The consequence is modification of surface morphology, variation in polymer chain organization, and change of molecular nature during the formation of TFC membranes [28]. Based on the results obtained from the FO test, it can be concluded that 3 wt% DMSO is the optimal additive for the TFC membrane, which results in higher water flux ($13.97 \pm 0.20 \text{ L m}^{-2} \text{ h}^{-1}$) and lower reverse salt flux ($1.15 \pm 0.13 \text{ g m}^{-2} \text{ h}^{-1}$) among those additives. Nevertheless, the addition of PIP resulted in a negative effect on the water flux, which may be attributed to the participation of PIP in IP reaction, the participation of PIP leads to the formation of barrier layer with maximum thickness at low concentration of PIP. Further increase in PIP concentration can lead to the accumulation of PIP in the amino and group rich region of the thin film and increase the density of the film [4,55,56]. The reverse salt flux of the TFC membranes with the varying

amounts of additives was shown in Fig. 6(b), the introduction of the four additives promoted the salt rejection performance.

In order to further study the effect of four additives on PA layer structures and properties. The ATR-FTIR spectra of the TFC membranes with the four additives and the estimated ratio of $I_{(-\text{COOH})}/I_{(-\text{CONH})}$ groups are presented in Fig. 7. The detailed spectra in the range from $2,100$ to 400 cm^{-1} (Fig. 7(a)) reveal little change with the introduction of four additives, suggesting the degree of influence of additives in MPD solution on the PA layer is less than that of the organic solvents.

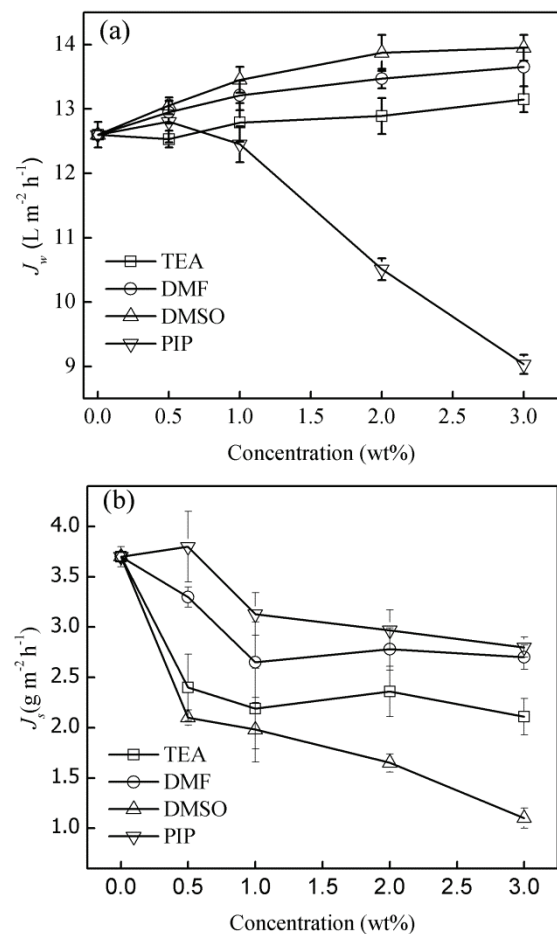


Fig. 6. Performance of PA TFC membranes with different concentration additives in the MPD solution.

Table 2

Analysis of the water permeability (A), salt permeability (B), structural parameter (S), hydrophilicity and surface energy of the TFC membranes with 1 wt% additives in the MPD solution

Additives	A (L m ⁻² h ⁻¹ bar ⁻¹)	B (L m ⁻² h ⁻¹)	S (μm)	Contact angle (deg)	$-\Delta G_{\text{SL}}$ (mJ m ⁻²)	γ_s^{LW} (mN m ⁻¹)
None	0.638	0.161	363	79.55 ± 0.85	41.41	24.84
TEA	0.641	0.137	265	64.07 ± 1.03	59.36	35.24
DMF	0.679	0.143	288	62.80 ± 0.76	59.86	34.38
DMSO	0.692	0.131	257	67.41 ± 0.95	44.75	32.59
PIP	0.485	0.128	212	66.53 ± 1.17	48.58	29.37

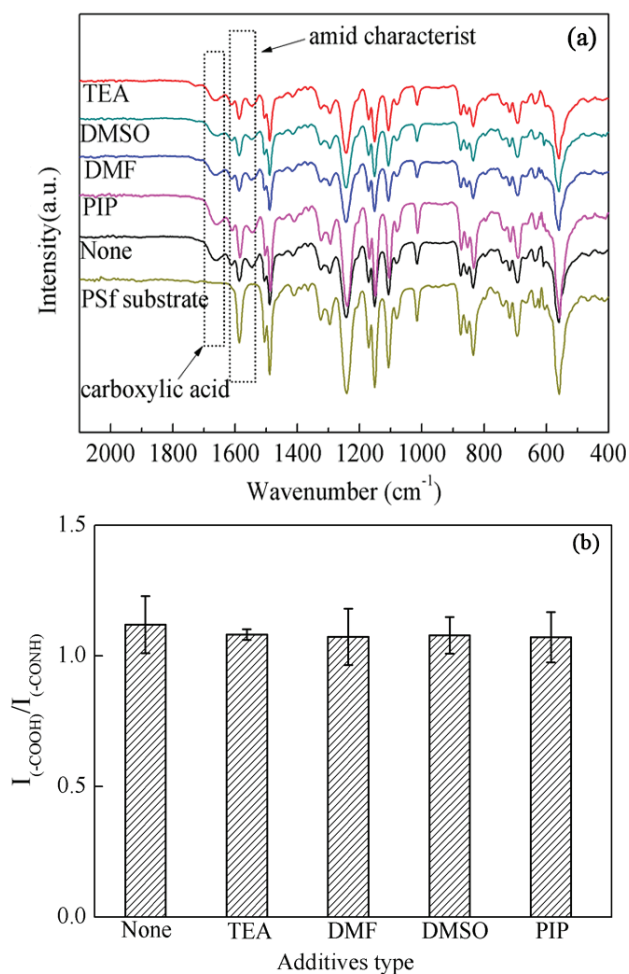


Fig. 7. (a) ATR-FTIR spectra and (b) the estimated ratio of (-COOH)/(-COONH) groups of the PA TFC membranes with 1 wt% additives in the MPD solution.

4. Conclusions

Here we focus on the effect of the types of both organic solvent and aqueous-phase additive on the PA layer of TFC membranes specifically tailored in FO process. Among the four types of organic solvents, the hexane-based PA TFC membrane shows higher water flux, hydrophilicity and lower crosslinking degree compared with other membranes. Higher heat-curing temperature is beneficial for improving salt rejection of the TFC membrane. The addition of four aqueous-phase additives leads to formation of a more hydrophilic PA layer. The water flux of TFC membranes increases after adding 3 wt% DMSO into the MPD solution, with a sharp decrease of reverse salt flux. In short, the present work has demonstrated that the introduction of additives into MPD solution is promising for TFC FO membranes.

Acknowledgment

This work was financially supported by “the National Science Foundation of China” (Grant No. 21376030).

References

- [1] P. Lu, S. Liang, T. Zhou, X. Mei, Y. Zhang, C. Zhang, A. Umar, H. Wang, Q. Wang, Typical thin-film composite (TFC) membranes modified with inorganic nanomaterials for forward osmosis: a review, *Nanosci. Nanotechnol. Lett.*, 8 (2016) 906–916.
- [2] J.J. Qin, W.C.L. Lay, K.A. Kekre, Recent developments and future challenges of forward osmosis for desalination: a review, *Desal. Wat. Treat.*, 39 (2012) 123–136.
- [3] T.Y. Cath, A.E. Childress, M. Elimelech, Forward osmosis: principles, applications, and recent developments, *J. Membr. Sci.*, 281 (2006) 70–87.
- [4] N.K. Saha, S.V. Joshi, Performance evaluation of thin film composite polyamide nanofiltration membrane with variation in monomer type, *J. Membr. Sci.*, 342 (2009) 60–69.
- [5] T. Sasaki, H. Fujimaki, T. Uemura, M. Kurihara, Interfacially Synthesized Reverse Osmosis Membrane, US Patent number 4,277,344, 1981.
- [6] K.P. Lee, T.C. Arnot, D. Mattia, A review of reverse osmosis membrane materials for desalination—development to date and future potential, *J. Membr. Sci.*, 370 (2011) 1–22.
- [7] W.J. Lau, A.F. Ismail, N. Misdan, M.A. Kassim, A recent progress in thin film composite membrane: a review, *Desalination*, 287 (2012) 190–199.
- [8] D. Li, Y. Yan, H. Wang, Recent advances in polymer and polymeric composite membranes for reverse and forward osmosis processes, *Prog. Polym. Sci.*, 61 (2016) 104–155.
- [9] J. Wei, C. Qiu, C.Y. Tang, R. Wang, A.G. Fane, Synthesis and characterization of flat-sheet thin film composite forward osmosis membranes, *J. Membr. Sci.*, 372 (2011) 292–302.
- [10] P.H. Duong, S. Chisca, P.Y. Hong, H. Cheng, S.P. Nunes, T.S. Chung, Hydroxyl functionalized polytriazole-copolyoxadiazole as substrates for forward osmosis membranes, *ACS Appl. Mater. Interfaces*, 7 (2015) 3950–3973.
- [11] P. Sukitpaneevit, T.S. Chung, High performance thin-film composite forward osmosis hollow fiber membranes with macrovoid-free and highly porous structure for sustainable water production, *Environ. Sci. Technol.*, 46 (2012) 7356–7365.
- [12] W. Fang, R. Wang, S. Chou, L. Setiawan, A.G. Fane, Composite forward osmosis hollow fiber membranes: integration of RO- and NF-like selective layers to enhance membrane properties of anti-scaling and anti-internal concentration polarization, *J. Membr. Sci.*, 394–395 (2012) 140–150.
- [13] N.N. Bui, J.R. Mccutcheon, Hydrophilic nanofibers as new supports for thin film composite membranes for engineered osmosis, *Environ. Sci. Technol.*, 47 (2012) 1761–1769.
- [14] R.W. Baker, *Membrane Technology and Applications*, 3rd ed., Wiley, New York, 2012, pp. 97–247.
- [15] R.J. Petersen, Composite reverse osmosis and nanofiltration membranes, *J. Membr. Sci.*, 83 (1993) 81–150.
- [16] R.X. Zhang, J. Vanneste, L. Poelmans, B.V.D. Bruggen, Effect of the manufacturing conditions on the structure and performance of thin-film composite membranes, *J. Appl. Polym. Sci.*, 125 (2012) 3755–3769.
- [17] S.H. Maruf, A.R. Greenberg, J. Pellegrino, Y. Ding, Fabrication and characterization of a surface-patterned thin film composite membrane, *J. Membr. Sci.*, 452 (2014) 11–19.
- [18] C.Y. Tang, Y.N. Kwon, J.O. Leckie, Effect of membrane chemistry and coating layer on physiochemical properties of thin film composite polyamide RO and NF membranes: II. Membrane physiochemical properties and their dependence on polyamide and coating layers, *Desalination*, 242 (2009) 168–182.
- [19] A.K. Ghosh, B.H. Jeong, X. Huang, E.M.V. Hoek, Impacts of reaction and curing conditions on polyamide composite reverse osmosis membrane properties, *J. Membr. Sci.*, 311 (2008) 34–45.
- [20] T. Kamada, T. Ohara, T. Shintani, T. Tsuru, Controlled surface morphology of polyamide membranes via the addition of co-solvent for improved permeate flux, *J. Membr. Sci.*, 467 (2014) 303–312.
- [21] I.C. Kim, J. Jegal, K.H. Lee, Effect of aqueous and organic solutions on the performance of polyamide thin-film-composite nanofiltration membranes, *J. Polym. Sci., Part B: Polym. Phys.*, 40 (2002) 2151–2163.

- [22] I.C. Kim, B.R. Jeong, S.J. Kim, K.H. Lee, Preparation of high flux thinfilm composite polyamide membrane: the effect of alkyl phosphate additives during interfacial polymerization, *Desalination*, 308 (2013) 111–114.
- [23] C. Kong, M. Kanazashi, T. Yamamoto, T. Shintani, T. Tsuru, Controlled synthesis of high performance polyamide membrane with thindense layer for water desalination, *J. Membr. Sci.*, 362 (2010) 76–80.
- [24] C. Klaysom, S. Hermans, A. Gahlaut, S. Van Craenenbroeck, I. Vankelecom, Polyamide/polyacrylonitrile (PA/PAN) thin film composite osmosis membranes: film optimization, characterization and performance evaluation, *J. Membr. Sci.*, 445 (2013) 25–33.
- [25] F. Yan, H. Chen, Y. Lu, Z. Lu, S. Yu, M. Liu, C. Gao, Improving the water permeability and antifouling property of thin-film composite polyamide nanofiltration membrane by modifying the active layer with triethanolamine, *J. Membr. Sci.*, 513 (2016) 108–116.
- [26] A.P. Rao, N.V. Desai, R. Rangarajan, Interfacially synthesized thin film composite RO membranes for seawater desalination, *Appl. Polym.*, 10 (2016) 44130.
- [27] M.A. Kuehne, R.Q. Song, N.N. Li, W.W.S. Ho, R.J. Petersen, Flux Enhancement in TFC RO Membranes, Joint China/USA Chemical Engineering Conference, 20 (2000) 23–26.
- [28] F. Wu, X. Liu, C. Au, Effects of DMSO and glycerol additives on the property of polyamide reverse osmosis membrane, *Water Sci. Technol.*, 74 (2016) 1619–1625.
- [29] P. Gorgojo, M.F. Jimenez-Solomon, A.G. Livingston, Polyamide thin film composite membranes on cross-linked polyimide supports: improvement of RO performance via activating solvent, *Desalination*, 344 (2014) 181–188.
- [30] X. Lu, L.H.A. Chavez, J. Ma, M. Elimelech, Influence of active layer and support layer surface structures on organic fouling propensity of thin-film composite forward osmosis membranes, *Environ. Sci. Technol.*, 49 (2015) 1436–1444.
- [31] Y. Cui, X.Y. Liu, T.S. Chung, Ultrathin polyamide membranes fabricated from free-standing interfacial polymerization: synthesis, modifications and post-treatment, *Ind. Eng. Chem. Res.*, 56 (2017) 513–523.
- [32] C.J. van Oss, Development and applications of the interfacial tension between water and organic or biological surfaces, *Colloids Surf., B*, 54 (2007) 2–9.
- [33] G.N. Lewis, Valence and the structure of atoms and molecules, *Phys. Teach.*, 31 (1968) 435–443.
- [34] S. Liang, Y. Kang, A. Tiraferri, E.P. Giannelis, X. Huang, M. Elimelech, Highly hydrophilic polyvinylidene fluoride (PVDF) ultrafiltration membranes via postfabrication grafting of surface-tailored silica nanoparticles, *ACS Appl. Mater. Interfaces*, 5 (2013) 6694–6703.
- [35] F.M. Fowkes, Additivity of intermolecular forces at interfaces. I. determination of the contribution to surface and interfacial tensions of dispersion forces in various liquids, *J. Phys. Chem.*, 67 (1963) 2538–2541.
- [36] P. Lu, S. Liang, L. Qiu, Y. Gao, Q. Wang, Thin film nanocomposite forward osmosis membranes based on layered double hydroxide nanoparticles blended substrates, *J. Membr. Sci.*, 504 (2016) 196–205.
- [37] A. Docoslis, R.F. Giese, C.J.V. Oss, Influence of the water–air interface on the apparent surface tension of aqueous solutions of hydrophilic solutes, *Colloids Surf., B*, 19 (2000) 147–162.
- [38] G. Hurwitz, G.R. Guille, E.M.V. Hoek, Probing polyamide membrane surface charge, zeta potential, wettability, and hydrophilicity with contact angle measurements, *J. Membr. Sci.*, 349 (2010) 349–357.
- [39] A. Tiraferri, N.Y. Yip, A.P. Straub, S. Romero-Vargas Castrillon, M. Elimelech, A method for the simultaneous determination of transport and structural parameters of forward osmosis membranes, *J. Membr. Sci.*, 444 (2013) 523–538.
- [40] Y. Wang, X. Li, C. Cheng, Y. He, J. Pan, T. Xu, Second interfacial polymerization on polyamide surface using aliphatic diamine with improved performance of TFC FO membranes, *J. Membr. Sci.*, 498 (2016) 30–38.
- [41] P. Lu, S. Liang, T. Zhou, X. Mei, Y. Zhang, C. Zhang, A. Umarbc, Q. Wang, Layered double hydroxide/graphene oxide hybrid incorporated polysulfone substrate for thin-film nanocomposite forward osmosis membranes, *RSC Adv.*, 6 (2016) 56599–56609.
- [42] L.L. Xia, C.L. Li, Y. Wang, In-situ crosslinked PVA/organosilica hybrid membranes for pervaporation separations, *J. Membr. Sci.*, 498 (2016) 263–275.
- [43] S.H. Huang, Y.Y. Liu, Y.H. Huang, K.S. Liao, C.C. Hu, K.R. Lee, J.Y. Lai, Study on characterization and pervaporation performance of interfacially polymerized polyamide thin-film composite membranes for dehydrating tetrahydrofuran, *J. Membr. Sci.*, 470 (2014) 411–420.
- [44] V. Freger, S. Srebnik, Mathematical model of charge and density distributions in interfacial polymerization of thin films, *J. Appl. Polym. Sci.*, 88 (2003) 1162.
- [45] D. Go´mez-Dí´az, J.C. Mejuto, J.M. Navaza, Physicochemical properties of liquid mixtures. 1. Viscosity, density, surface tension and refractive index of cyclohexane +2,2,4-trimethylpentane binary liquid systems from 25°C to 50°C, *J. Chem. Eng. Data*, 46 (2001) 720–724.
- [46] N.N. Bui, M.L. Lind, E.M.V. Hoek, J.R. McCutcheon, Electrospun nanofiber supported thin film composite membranes for engineered osmosis, *J. Membr. Sci.*, 385–386 (2011) 10–19.
- [47] H. Wang, L. Li, X. Zhang, S. Zhang, Polyamide thin-film composite membranes prepared from a novel triamine 3,5-diamino-N-(4-aminophenyl)-benzamide monomer and m-phenylenediamine, *J. Membr. Sci.*, 353 (2010) 78–84.
- [48] P. Hajighahremanzadeh, M. Abbaszadeh, S.A. Mousavi, M. Soltanieh, H. Bakhshi, Polyamide/polyacrylonitrile thin film composites as forward osmosis membranes, *Appl. Polym.*, 10 (2016) 44130.
- [49] A. Idris, F. Kormin, M. Suput, The effect of curing temperature on the performance of thin film composite membrane, *J. Teknologi*, 43 (2005) 51–64.
- [50] I.J. Roh, J.J. Kim, S.Y. Park, Mechanical properties and reverse osmosis performance of interfacial polymerized polyamide thin films, *J. Membr. Sci.*, 197 (2002) 199–210.
- [51] D. Wu, S. Yu, D. Lawless, X. Feng, Thin film composite nanofiltration membranes fabricated from polymeric amine polyethylenimine imbedded with monomeric amine piperazine for enhanced salt separations, *React. Funct. Polym.*, 86 (2015) 168–183.
- [52] R. Ma, Y.L. Ji, X.D. Weng, Q.F. An, C.J. Gao, High-flux and fouling-resistant reverse osmosis membrane prepared with incorporating zwitterionic amine monomers via interfacial polymerization, *Desalination*, 381 (2016) 100–110.
- [53] A.L. Ahmad, B.S. Ooi, Optimization of composite nanofiltration membrane through pH control: application in CuSO₄ removal, *Sep. Purif. Technol.*, 47 (2006) 162–172.
- [54] P.W. Morgan, S.L. Kwolek, Interfacial polycondensation. II. Fundamentals of polymer formation at liquid interfaces, *Polym. Sci.*, 34 (1996) 531–559.
- [55] R. Nadler, S. Srebnik, Molecular simulation of polyamide synthesis by interfacial polymerization, *J. Membr. Sci.*, 315 (2008) 100–105.
- [56] D.J. Mohan, L. Kullová, A study on the relationship between preparation condition and properties/performance of polyamide TFC membrane by IR, DSC, TGA, and SEM techniques, *Desal. Wat. Treat.*, 51 (2013) 586–596.